

Adaptive Histogram Equalization Based Image Forensics Using Statistics of DC DCT Coefficients

Neetu SINGH, Abhinav GUPTA, Roop Chand JAIN

Department of Electronics and Communication Engineering, Jaypee Institute of Information Technology, Sector-62, Noida, Uttar Pradesh 201309, India

neetu.singh@jiit.ac.in, abhinav.gupta@jiit.ac.in, rc.jain@jiit.ac.in

DOI: 10.15598/aeee.v16i1.2647

Abstract. *The vulnerability of digital images is growing towards manipulation. This motivated an area of research to deal with digital image forgeries. The certifying origin and content of digital images is an open problem in the multimedia world. One of the ways to find the truth of images is finding the presence of any type of contrast enhancement. In this work, novel and simple machine learning tool is proposed to detect the presence of histogram equalization using statistical parameters of DC Discrete Cosine Transform (DCT) coefficients. The statistical parameters of the Gaussian Mixture Model (GMM) fitted to DC DCT coefficients are used as features for classifying original and histogram equalized images. An SVM classifier has been developed to classify original and histogram equalized image which can detect histogram equalized image with accuracy greater than 95 % when false rate is less than 5 %.*

Keywords

CLAHE, DC DCT coefficients, Gaussian Mixture Model, image forensics.

1. Introduction

Digital images are generally used to establish the occurrence of some man-made or natural incidents. These days images are one of the biggest and largest means of communication through different media and often required authenticity test. The availability of a large number of software products in multimedia devices is making creation and manipulation of digital images very cheap and convenient. Digital images can be manipulated by tampering source of information and/or the content of information. Research area which cov-

ers finding origin and authenticity of an image is known as Digital Image Forensics (DIF) [1], [2] and [3]. The forensics of source involves finding camera or source from which an image is generated or captured, and the forensics of authentication involves finding traces of manipulation in an image. To create invincible tampered images, sampling, interpolation, contrast enhancement, median filtering, addition of noise and saving in lossy compression format are some examples of the commonly involved techniques. These methods alone or chain of these methods are not tampering techniques, but they are required in order to hide any visual traces of the tampering. Therefore, detection of the presence of any such operation leads to the detail investigation of an image.

In literature of contrast enhancement-based DIF, mainly two types of classical contrast enhancements, such as power-law transformation and Global Histogram Equalization (GHE), are considered [4], [5], [6], [7], [8], [9] and [10]. In our work, we have focused on detection of histogram equalization operation. The GHE increases the global contrast of an image by equally distributing intensity levels. But these days, Adaptive Histogram Equalization (AHE) [11] and [12] is getting popular due to its performance in comparison to Global Histogram Equalization (GHE). In AHE, an image is divided into tiles and thereafter, HE is applied to each tile which leads to enhancement of smaller details by increasing local contrast of the image. The equalization process is followed by bilinear interpolation to smooth out the boundaries due to the tiling of images. Although, this provides better enhancement than global counterpart, enhancement of noise content in homogeneous regions of background is a major concern. Generally, various versions of AHE are available to suppress the enhanced noise [11]. The most popular and acceptable variation of AHE is contrast limited AHE (CLAHE) [12], [13], [14], [15] and [16]. The

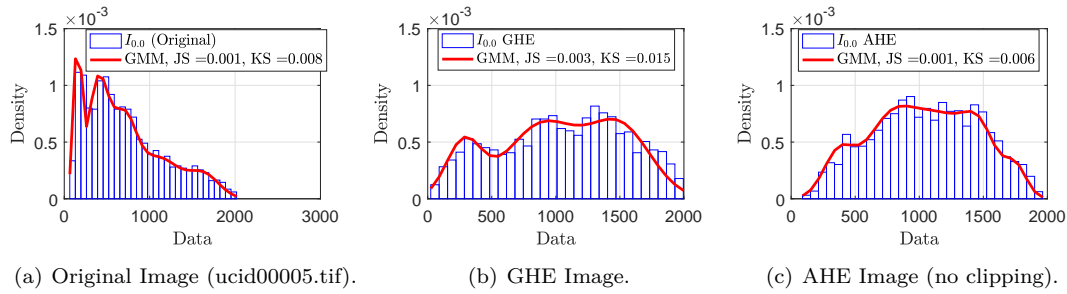


Fig. 1: Characterization of $I_{0,0}$ using GMM.

CLAHE suppresses enhancement of noise by limiting the highest value in image histogram known as Clip Limit (CL). The CL can be defined as highest value allowed in a bin of histogram of an image tile. The density values which are greater than CL in a given image tile are redistributed. The CL and number of tiles (T) are two important parameters of CLAHE. In literature, it is stated that different probability density functions (pdfs) (uniform, exponential, Rayleigh, etc.) for image histograms in HE for CLAHE are considered based on applications. In addition to natural images [16] and [17], CLAHE also found its application in enhancement of medical images [13] and [14] and underwater images [15].

Since the use of CLAHE is spreading, the tools to detect the presence of AHE are also required. In this paper, the statistical characterization of block DC coefficient of $2D \ 8 \times 8$ DCT coefficients is employed to classify original and HE images. HE images include GHE, AHE and CLAHE images. The block DC coefficient of $2D \ 8 \times 8$ DCT coefficients is defined as an array made up of all DC coefficients from 8×8 block of DCT coefficients. In image forensics, the DCT coefficient analysis is employed to detect tampering in JPEG compressed images [18] and [19]. Further, the statistical characterization of DCT coefficients has been popular for improvements in encoder/decoder for JPEG standard [20], [21], [22] and [23]. It may be noted that statistical characterization of block variance and AC DCT coefficients are recently employed to detect global contrast enhancement (or power-law transformation) [24].

In this work, a tool is developed using statistical parameters obtained from fitting of block DC coefficient by Gaussian Mixture Model (GMM). The estimated parameters with other statistical parameters are applied to train a 10-fold cross-validation Support Vector Machine (SVM) [25]. The trained SVM classifier can be used to classify original and HE images. The proposed tool is independent of T and can detect the presence of HE for a large set of CL , all considered pdfs (uniform distribution, exponential distribution, Rayleigh distribution) for image histograms and range

of gray levels ("full" and "original") used for equalization. By means of Receiver operating curves (ROC), the efficacy of the proposed tool for the classification of original and HE images is shown. Additionally, the performance of the tool in detection of CLAHE images for different CL s, T s, image histogram equalization pdfs, and range of gray levels used in equalization is also discussed.

The paper is divided into four sections. Section 2. describes the statistical characterization of block DC DCT coefficients by GMM. The HE detection system and its detection algorithm with ROC curves of developed classifiers are explained in Sec. 3. Section 4. concludes the paper.

2. Statistical Characterization of DC DCT Coefficients

The block DC DCT coefficients obtained by employing type - II DCT are characterized using GMM in order to classify original and HE images.

2.1. Gaussian Mixture Model

A GMM is a pdf which is the weighted sum of densities of Gaussian components defined as

$$p\left(x|\mu_i, \sum_i, w_i\right) = \sum_{i=1}^K w_i g\left(x|\mu_i, \sum_i\right), \quad (1)$$

where x is D-dimensional continuous-valued data vector, w_i for $i = 1, 2, 3, \dots, K$ are the weights of mixture and K is the number of components. In Eq. (1), g is a D-dimensional Gaussian density which can be expressed as

$$g\left(x|\mu_i, \sum_i\right) = \frac{1}{2\pi^{(D/2)} |\sum_i|^{(1/2)}} \exp\left\{-\frac{1}{2} X' \sum_i^{-1} X\right\}, \quad (2)$$

where $X = (x - \mu_i)$, μ_i is mean vector, and \sum_i is covariance matrix. It may be observed from Eq. (1), the sum of mixture weights (w_i) for all components

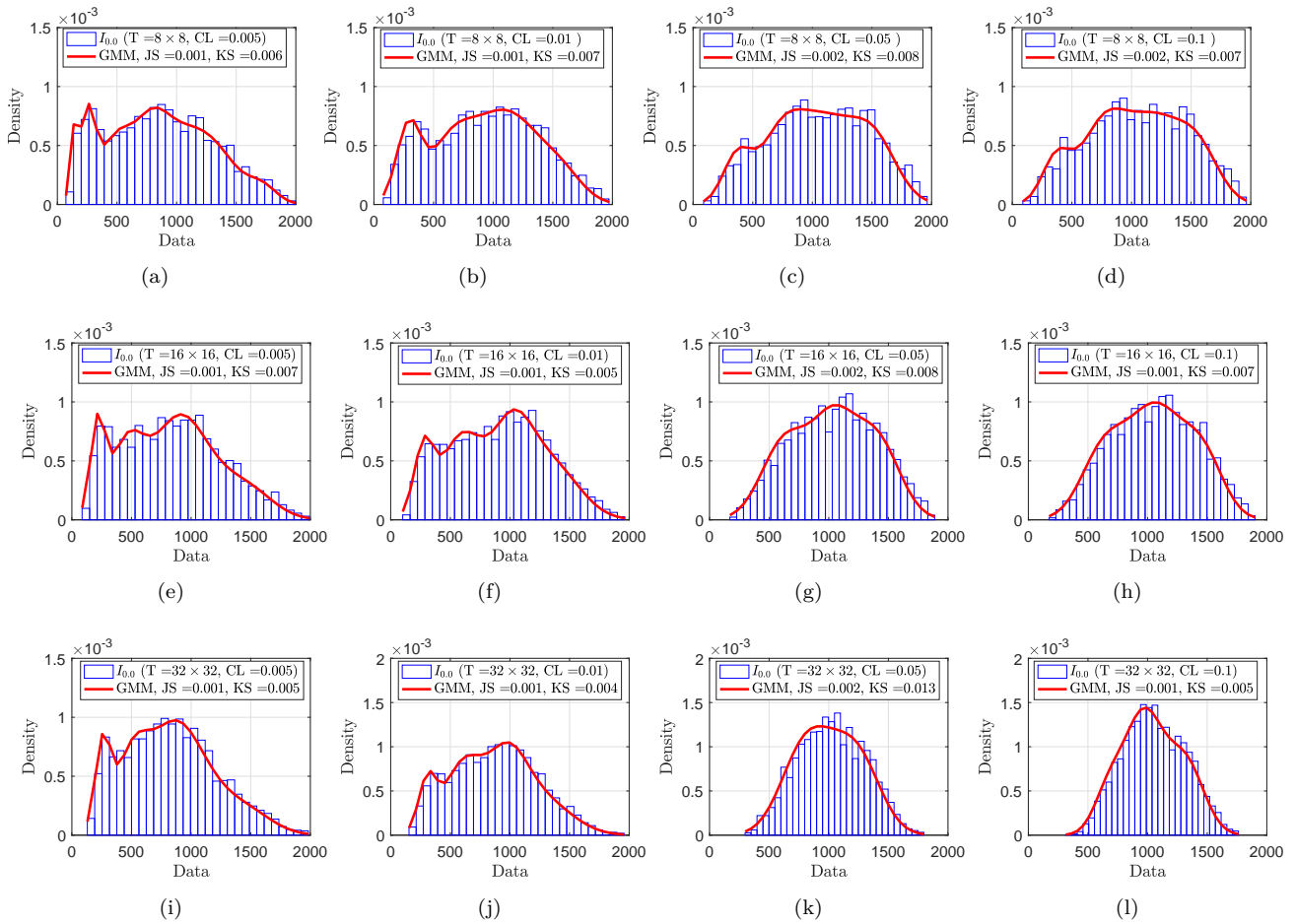


Fig. 2: Characterization of $I_{0,0}$ of CLAHE images using GMM with varying CL and T (a), (e) and (i) $CL = 0.005$, (b), (f) and (j) $CL = 0.01$, (c), (g) and (k) $CL = 0.05$, (d), (h) and (l) $CL = 0.1$. (a)-(d) $T = 8 \times 8$, (e)-(h) $T = 16 \times 16$, and (i)-(l) $T = 32 \times 32$, represents number of tiles used in CLAHE with uniform pdf and "full" range of gray levels.

is equals to 1. The parameters of GMM are: mean vector, covariance matrix, and mixture weights. These parameters can be collected to form a feature set (θ) given by,

$$\theta = \left\{ w_i, \mu_i, \sum_i \right\}, i = 1, 2, 3, \dots, K. \quad (3)$$

The model settings, like the number of components, type of covariance matrix, and sharing of parameters, depends on the size of available data for estimation of parameters and application. In our work, the diagonal covariance matrix for all components is used, and the parameters in Eq. (3) are estimated using Maximum Likelihood Estimation (MLE).

2.2. Statistical Characterization

The DC coefficients of images are calculated in grayscale domain by employing type - II 8×8 block DCT of JPEG standard. The type-II DCT is defined

$$I_{u,v}^b = \alpha_u(u)\alpha_v(v) \sum_{x=0}^7 \sum_{y=0}^7 i_{x,y} \cos\left(\frac{\pi(2x+1)u}{16}\right) \cos\left(\frac{\pi(2y+1)v}{16}\right), \quad (4)$$

where x, y and u, v represent spatial and frequency domain variables, respectively. The value of $\alpha_u(u)$ and $\alpha_v(v)$ at $u = 0, v = 0$ is $1/\sqrt{8}$. The DCT coefficient at $u = 0, v = 0$ is known as DC coefficient which is defined in type - II DCT as

$$I_{0,0}^b = \frac{1}{8} \sum_{x=0}^7 \sum_{y=0}^7 i_{x,y}, \quad (5)$$

where $I_{0,0}^b$ is the DC coefficient of an image block, b represents number of the block. It may be noted that $I_{0,0}^b$ is eight times of the mean value of 8×8 block of an image. The block DC coefficient $I_{0,0}$ can be defined as

$$I_{0,0} = \{I_{0,0}^1, I_{0,0}^2, \dots, I_{0,0}^B\}, \quad (6)$$

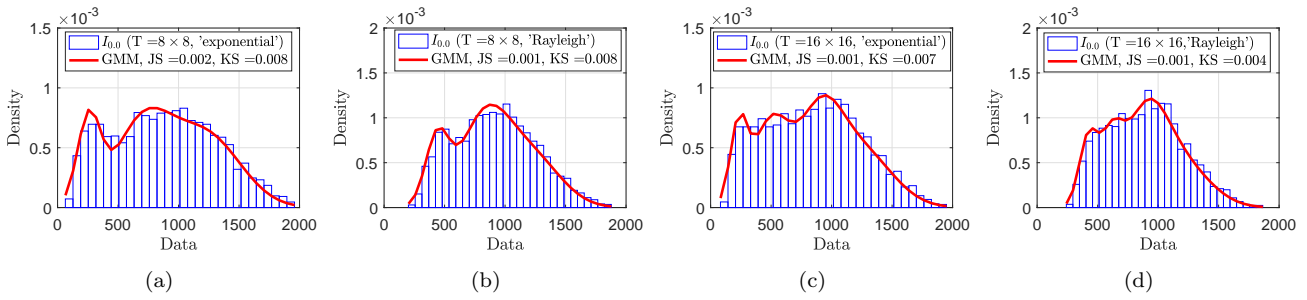


Fig. 3: Characterization of $I_{0,0}$ of CLAHE images using GMM for (a) $T = 8 \times 8$, exponential distribution (b) $T = 8 \times 8$, Rayleigh distribution, (c) $T = 16 \times 16$, exponential distribution and (d) $T = 16 \times 16$, Rayleigh distribution with $CL = 0.01$ and "full" range of gray levels.

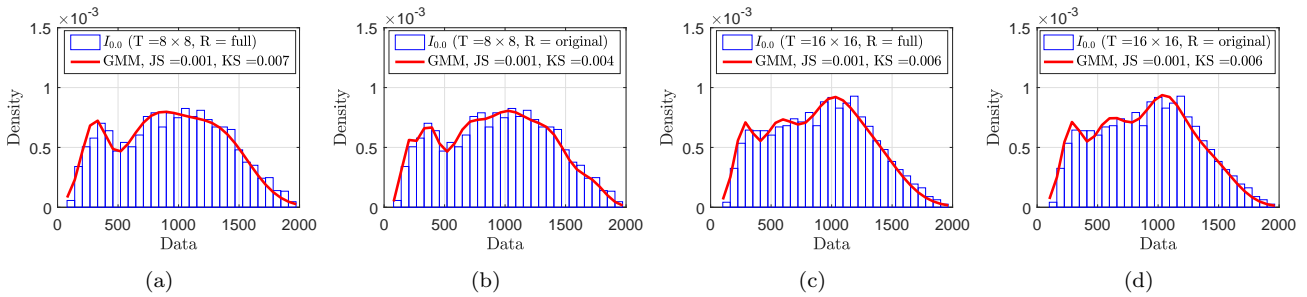


Fig. 4: Characterization of $I_{0,0}$ of CLAHE images using GMM for (a) $T = 8 \times 8$, "full" range (b) $T = 8 \times 8$, "original" range, (c) $T = 16 \times 16$, "full" range and (d) $T = 16 \times 16$, "original" range with $CL = 0.01$ and uniform distribution.

where B is number of 8×8 non-overlapping blocks in the input image. The histograms of $I_{0,0}$ of original image, histogram equalized image, and adaptive histogram equalized image are characterized by GMM as shown in Fig. 1. The statistical characterization of $I_{0,0}$ of CLAHE images for different values of CL and T is shown in Fig. 2. The statistical characterization of $I_{0,0}$ of CLAHE images for different pdfs of histograms is shown in Fig. 3. The effect of the range of gray levels on characterization of $I_{0,0}$ is shown in Fig. 4. In the legend of Fig. 4, "full" represents the entire available range of gray levels (i.e., 256 for 8-bit image), and "original" represents the range of gray levels in original image. The characterizations shown in Fig. 1, Fig. 2, Fig. 3 and Fig. 4 are obtained with optimum number of components found using Akaike Information Criterion (AIC) [26]. Further, to measure the efficacy of characterization, we have employed Jensen-Shannon (JS) divergence [27] and [28] and Kolmogorov-Smirnov (KS) statistic [29] and [28]. The values of JS and KS in different cases of HE for a UCID [30] image are shown in legends of Fig. 1, Fig. 2, Fig. 3 and Fig. 4. A consistency in values of JS and KS concludes GMM as a good model of fit across original and different types of HE images.

2.3. Parameter Analysis of CLAHE

To find the optimum number of components (K) for GMM, we have calculated the mean JS and KS values with varying K (1, 3, 5, ..., 10) for all 1338 images of UCID database. It is worth mentioning that KS hypothesis test is performed with $\alpha = 0.01$. The efficacy of GMM for characterization of $I_{0,0}$ can be observed from Tab. 1, Tab. 2, Tab. 3, Tab. 4 and Tab. 5.

Effect of CL : With an increase in the value of CL from 0.005 (large clipping) to 1 (no clipping), the shift in skewness from right to left of $p(I_{0,0})$ is observed (Fig. 2 and Fig. 3). Lower values of CL represent low contrast, and higher values of CL represent higher contrast. Additionally, a decrease in kurtosis among distributions can also be observed in Fig. 3. The effect of CL in characterization of $p(I_{0,0})$ is tabulated in Tab. 1, Tab. 2, Tab. 3 and Tab. 4 for different values of T .

Effect of T : The effect of the number of tiles T used in CLAHE is shown in Fig. 2. It may be observed from Fig. 2 that kurtosis of $p(I_{0,0})$ increases with increase of T . The Tab. 1, Tab. 2, Tab. 3 and Tab. 4 show variation of up to 2% in mean JS and KS statistic values with varying T .

Tab. 1: Mean values of JS and KS and KS Hypothesis result for $T = 8 \times 8$ (Org = Original).

CL	1C			3C			5C			10C		
	JS	KS	KS Hypo									
Org	0.0606	0.1683	2.39	0.0122	0.0395	71.52	0.0110	0.0441	80.12	0.0203	0.0813	75.86
0.005	0.0371	0.1185	7.55	0.0129	0.0439	85.13	0.0134	0.0497	86.62	0.0210	0.0816	76.83
0.01	0.0267	0.0944	14.72	0.0117	0.0412	89.24	0.0173	0.0603	89.61	0.0265	0.0919	87.44
0.05	0.0113	0.0528	40.96	0.0155	0.0528	94.25	0.0254	0.0829	92.83	0.0322	0.1046	91.33
0.1	0.0084	0.0438	52.84	0.0192	0.0644	93.2	0.0319	0.1028	92.53	0.0392	0.1258	90.66
1	0.0067	0.0378	63.45	0.0254	0.0834	93.2	0.039	0.1243	92.15	0.0448	0.1421	90.96

Tab. 2: Mean values of JS and KS and KS Hypothesis result for $T = 16 \times 16$.

CL	1C			3C			5C			10C		
	JS	KS	KS Hypo									
Org	0.0606	0.1683	2.39	0.0121	0.0395	71.52	0.0098	0.0408	79.82	0.0176	0.0728	75.26
0.005	0.0409	0.1216	8	0.0105	0.0366	85.35	0.0126	0.0472	85.8	0.0215	0.0792	82.29
0.01	0.0311	0.0993	14.5	0.0096	0.0341	90.06	0.0123	0.0444	88.94	0.0218	0.0774	85.65
0.05	0.0132	0.0561	45.52	0.0186	0.0630	92.9	0.0264	0.0868	92.38	0.0301	0.0985	91.55
0.1	0.0089	0.0431	60.24	0.0235	0.0782	92.97	0.0319	0.1038	91.85	0.0393	0.1269	90.21
1	0.0057	0.0322	76.46	0.0329	0.1075	93.27	0.0391	0.1256	92.08	0.0473	0.1507	90.28

Tab. 3: Mean values of JS and KS and KS Hypothesis result for $T = 32 \times 32$.

CL	1C			3C			5C			10C		
	JS	KS	KS Hypo	JS	KS	KS Hypo	JS	KS	KS Hypo	JS	KS	KS Hypo
Org	0.0606	0.1684	2.39	0.0121	0.0388	71.52	0.0098	0.0408	79.82	0.0229	0.0899	74.89
0.005	0.0482	0.1247	8.45	0.0148	0.0532	73.84	0.0192	0.0750	76.08	0.0321	0.1231	71.52
0.01	0.0413	0.1087	15.02	0.0135	0.0493	80.57	0.0224	0.0839	80.42	0.0324	0.1186	76.83
0.05	0.0201	0.0642	39.69	0.0202	0.0676	93.05	0.0280	0.0925	92.3	0.0368	0.1216	90.58
0.1	0.0130	0.0515	51.05	0.0271	0.0897	92.3	0.0321	0.1049	91.63	0.0421	0.1373	90.21
1	0.0063	0.0333	70.7	0.0418	0.1357	90.88	0.0474	0.1529	89.46	0.0522	0.1676	87.74

Tab. 4: Mean values of JS and KS and KS Hypothesis result for $T = 64 \times 64$.

CL	1C			3C			5C			10C		
	JS	KS	KS Hypo									
Org	0.0606	0.1683	2.39	0.0125	0.0396	71.75	0.0107	0.0424	80.49	0.0237	0.0927	75.11
0.005	0.0438	0.1157	12.03	0.0164	0.0559	83.93	0.0234	0.0825	85.5	0.0339	0.1204	82.81
0.01	0.0438	0.1157	12.03	0.0164	0.0553	83.71	0.0244	0.0853	85.8	0.0313	0.1116	83.41
0.05	0.0332	0.0903	23.54	0.0199	0.0662	92.68	0.0286	0.0950	92.08	0.0401	0.1329	90.28
0.1	0.0252	0.0757	36.62	0.0255	0.0849	92.68	0.0338	0.1117	90.73	0.0411	0.1353	89.39
1	0.0129	0.0513	53.36	0.0307	0.1018	91.78	0.0392	0.1284	89.39	0.0444	0.1449	87

Tab. 5: Mean values of JS and KS and KS Hypothesis result for image HE pdfs ($D_1 =$ uniform distribution, $D_2 =$ exponential distribution and $D_3 =$ Rayleigh distribution) and range of gray levels ($R_1 =$ "full" and $R_2 =$ "original").

		1C			3C			5C			10C		
		JS	KS	KS Hypo	JS	KS	KS Hypo	JS	KS	KS Hypo	JS	KS	KS Hypo
D_1	R_1	0.027	0.094	14.72	0.012	0.041	89.24	0.017	0.060	89.61	0.026	0.092	87.44
	R_2	0.028	0.1	12.11	0.013	0.045	88.12	0.017	0.060	88.49	0.023	0.082	86.17
D_2	R_1	0.028	0.102	9.72	0.01	0.036	89.61	0.017	0.059	89.01	0.026	0.089	87.14
	R_2	0.029	0.108	8.37	0.012	0.0419	87.37	0.018	0.064	87.59	0.027	0.093	85.28
D_3	R_1	0.025	0.092	13.83	0.015	0.0514	92.08	0.023	0.075	92	0.029	0.095	89.91
	R_2	0.025	0.094	13.38	0.014	0.0465	92.08	0.021	0.071	91.93	0.033	0.1081	89.24

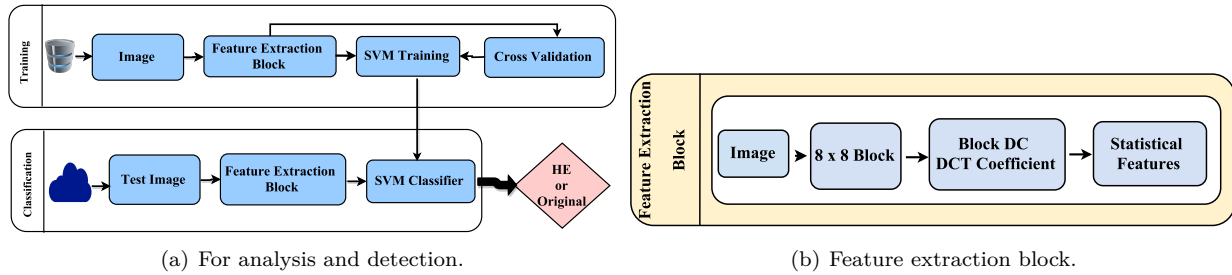


Fig. 5: The system model.

Effect of image HE pdfs: As may be observed from Tab. 5, the maximum number of KS hypothesis tests is passed when the image histogram equalization pdf is a Rayleigh distribution.

Effect of range of gray levels in HE: The mean values of JS and KS statistic are the smallest (Tab. 5) when the chosen gray levels are in full range with uniform and exponential distribution. But in case of Rayleigh distribution, the chosen ranges of gray levels have no effect on the mean values of JS and KS statistics.

One can observe from Tab. 1, Tab. 2, Tab. 3, Tab. 4 and Tab. 5 that the optimum values of JS and KS statistic are obtained with $K = 3$ and 5 . In our work, we have chosen $K = 5$ because the maximum number of KS hypothesis tests for original images is passed with $K = 5$. It is noteworthy that the mean values of JS and KS statistic are calculated after removing 5 % outliers from the original images database.

1. $I_{x,y}^t \leftarrow grayscale(I^t)$ where, $x = 0, 1, \dots, 7, y = 0, 1, \dots, 7$, represents spatial domain.
2. Compute 8×8 2D block DCT, $I_{u,v}^t \leftarrow DCT(I_{x,y}^t)$ where, $u = 0, 1, \dots, 7, v = 0, 1, \dots, 7$, represents frequency domain.
3. Compute the block DC Coefficient, $I_{0,0}^t$.
4. Estimate parameters by fitting block DC Coefficient, $I_{0,0}^t$ to GMM (Eq. 2).
5. Create features set, \mathbf{F} (Eq. 7).
6. $ghe \leftarrow SVMClassifier(\mathbf{F})$ here, $he = 0 \implies$ original and $he = 1 \implies$ HE.

Fig. 6: Proposed HE detection algorithm.

3. Histogram Equalization Detection

3.1. System Model for Analysis and Detection

The system model used for analysis and detection is shown in Fig. 5. The GHE, AHE and CLAHE operations are performed in spatial domain with 256 gray levels and saved in TIFF format. For CLAHE, the T are $8 \times 8, 16 \times 16, 32 \times 32$ and 64×64 and the CL are 0.005, 0.01, 0.03, 0.05, 0.07, 0.09, 0.1, 0.3. Additionally, the CLAHE images are also generated with exponentially and Rayleigh distributed histograms for all considered T s and CL s. For the range of gray levels in enhanced images, both "original" and "full" ranges are considered. For feature extraction (Fig. 5), the 2D 8×8 block DCT of the grayscale image is computed. The DC DCT coefficient of each block is collected to generate $I_{0,0}$ (Eq. 6). It is observed (Fig. 1, Fig. 2, Fig. 3, Fig. 4 and Fig. 5) that $p(I_{0,0})$ is varying with histogram equalization operations. Therefore, statistics of $I_{0,0}$ can be used as features for classification.

Construction of the feature set involves the calculation of 10 - fold cross-validation accuracies of SVM classifiers for respective feature set. The accuracies corresponding to different feature sets for classification between original and GHE, original and AHE, original and CLAHE ($CL = 0.05, D = D1, D2, D3, T = 8 \times 8, R1$) images are shown in Tab. 6. After experimentation, a 56-dimensional feature set \mathbf{F} Eq. (7) is constructed and used for classification between original and all types

Tab. 6: 10 – fold cross-validation accuracies of SVM classifiers for different feature sets.

Features	Number of features	Org vs. GHE	Org vs. AHE	Org vs. CLAHE (D1)	Org vs. CLAHE (D2)	Org vs. CLAHE (D3)
θ (Eq. 3)	15	86.7 %	88.7 %	86.1 %	83.8 %	87.6 %
S (Eq. 8)	11	98.8 %	97.0 %	93.8 %	92.0 %	93.1 %
$p(I_{0,0})$	30	95.7 %	97.4 %	93.0 %	91.9 %	93.6 %
$\theta + S$	26	97.4 %	97.4 %	93.7 %	92.0 %	94.0 %
F (Eq. 7)	56	97.7 %	98.6 %	95.4 %	94.3 %	96.1 %

of histogram operations. The estimated parameters from GMM are combined with mean, median, mode, variance, skewness, kurtosis, minimum, maximum, entropy, energy of $I_{0,0}$, number of peaks in $I_{0,0}$ and empirical $p(I_{0,0})$. The feature set F is defined as

$$F = \{\theta, p(I_{0,0}), S\}, \quad (7)$$

where

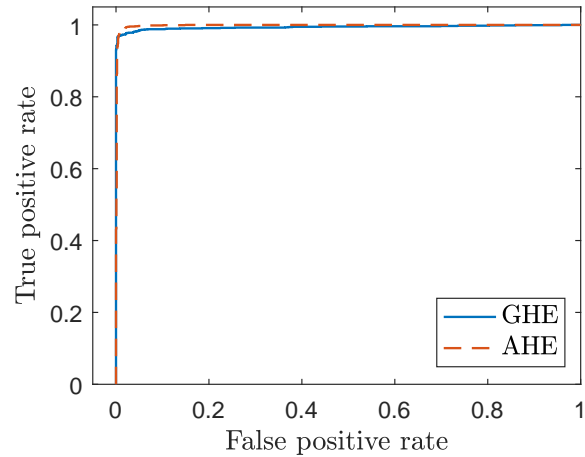
$$S = \left\{ \mu(I_{0,0}), \text{var}(I_{0,0}), \text{Sk}(I_{0,0}), \text{Ku}(I_{0,0}), \right. \\ \left. \text{min}(I_{0,0}), \text{max}(I_{0,0}), \text{median}(I_{0,0}), \text{mode}(I_{0,0}), \right. \\ \left. \text{energy}(I_{0,0}), \text{entropy}(I_{0,0}), \text{peaks}(I_{0,0}) \right\}. \quad (8)$$

The feature set Eq. (7) is applied to 10 – fold cross-validation SVM with Radial Basis Function (RBF) kernel for training.

3.2. Detection Algorithm and Results

The proposed detection algorithm for classifying original and histogram equalized images is shown in Fig. 6. To test the efficacy of the proposed algorithm with important parameters of GHE, AHE and CLAHE, we have created different simulation environments. The used database is UCID (TIFF format) with 1338 images. The performance of proposed classifiers is shown in Fig. 7, Fig. 8, Fig. 9, Fig. 10 and Fig. 11 using 10 – fold cross-validation ROC curves. The images are passed through GHE and AHE operation, and for preparation of feature matrix for each classification, the original images are mixed with corresponding HE images. The obtained ROC curves for classification between original and each GHE and AHE are shown in Fig. 7. The simulation environments used for CLAHE are tabulated in Tab. 7.

The achieved TPR is $> 95\%$ with $\text{FPR} < 5\%$ in most of the cases. The $CL = 0.005$ represents less contrast. Thus, the results at $CL = 0.005$ fall to 90% with exponential distribution. In case of GHE and AHE, detection accuracy is more than 99% with false alarm less than 1% , which is comparable to existing methods [6] and [9], as shown in Tab. 8. The detection results for AHE and CLAHE are not reported in [6] and [9]. The proposed method is applicable with high efficacy for all types of histogram equalization operations.

**Fig. 7:** ROC curves for GHE and AHE classifier.**Tab. 7:** Simulation environments of CLAHE. (D = distribution, D_1 = uniform distribution, D_2 = exponential distribution and D_3 = Rayleigh distribution) and R = range of gray levels, R_1 = "full" and R_2 = "original", "All" represents considered values of T and CL as described in Sec. 3.1.

Cases	Parameters		T	CL	D	R	ROC
	varying	constant					
Case 1		T	-	All	D_1	R_1	Fig. 8(a)
					D_2		Fig. 8(b)
					D_3		Fig. 8(c)
Case 2		CL	All	-	D_1	R_1	Fig. 9(a)
					D_2		Fig. 9(b)
					D_3		Fig. 9(c)
Case 3		D	All	All	-	R_1	Fig. 10
Case 4		R	All	All	All	-	Fig. 11

Tab. 8: Accuracy (TPR, FPR) of proposed method and existing methods in HE based image Forensics.

Methods	GHE	AHE and CLAHE
Stamm[6]	100 %, 3 %	NA
Yuan[9]	100 %, 1 %	NA
Proposed	99 %, 1 %	99 %, 1 % and 95 %, 5 %

4. Conclusion

The histogram equalization is a commonly used contrast enhancement technique. Its adaptive and contrast limited variant CLAHE is also spreading its footprint in application based image enhancements. We have developed a novel method to detect the presence of three commonly found

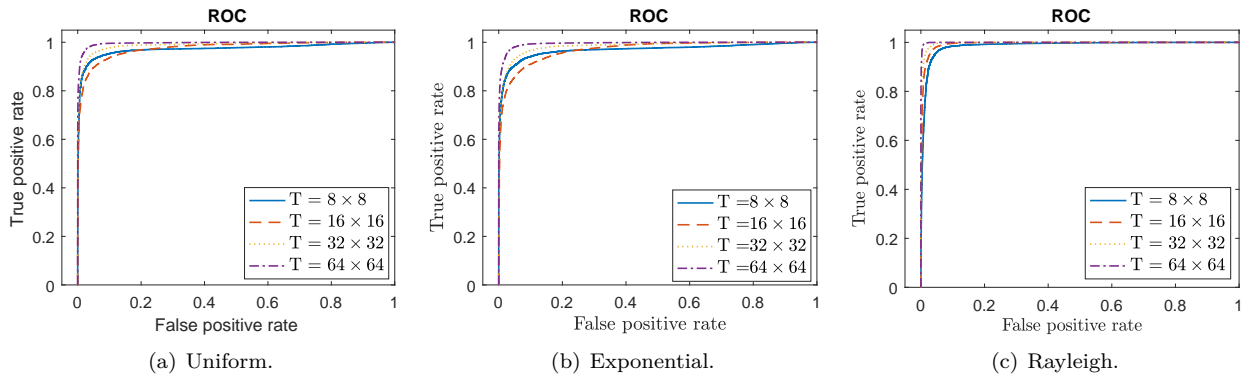


Fig. 8: ROC curves: HE detection for enhancement with varying T for all CL .

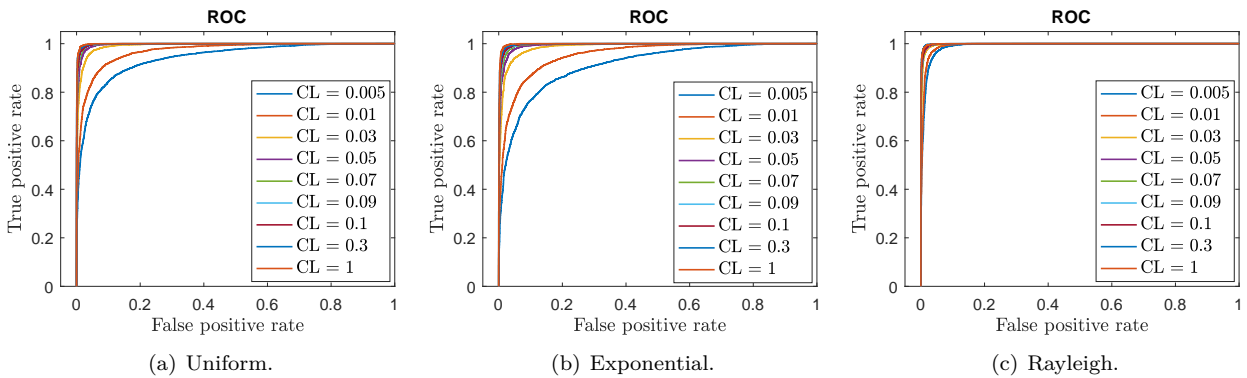


Fig. 9: ROC curves: HE detection for enhancement with varying CL for all T .

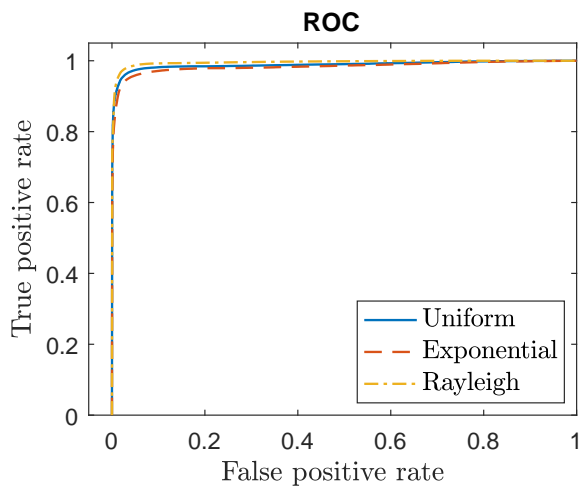


Fig. 10: ROC curves for different pdfs used in CLAHE.

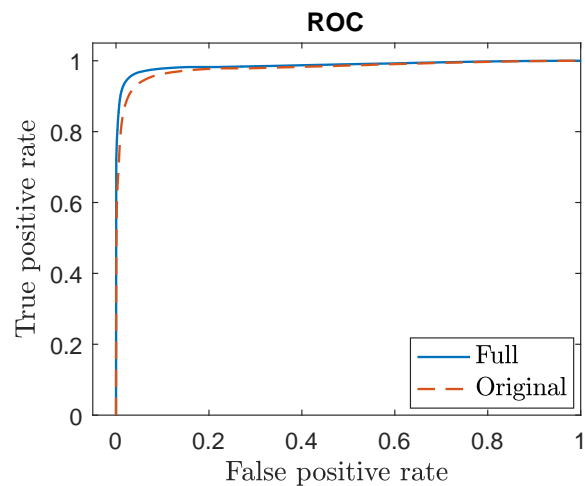


Fig. 11: ROC curves for different ranges used in CLAHE.

histogram equalization variants using statistical features. The proposed method employs statistical features of block DC coefficient to classify original and histogram equalized images. With few exceptions, the proposed tool achieves higher accuracy

with all variants of histogram equalization. This tool does not involve image histograms based methods for detection of contrast enhancement and involves DC DCT coefficients, which is least affected by JPEG compression after enhancement.

References

- [1] FARID, H. Image forgery detection. *IEEE Signal Processing Magazine*. 2009, vol. 26, iss. 2, pp. 16–25. ISSN 1053-5888. DOI: 10.1109/MSP.2008.931079.
- [2] REDL, J. A., W. TAKTAK and J. L. DUGELAY. Digital image forensics: a booklet for beginners. *Multimedia Tools and Applications*. 2011, vol. 51, iss. 1, pp. 133–162. ISSN 1573-7721. DOI: 10.1007/s11042-010-0620-1.
- [3] QAZI, T., K. HAYAT, S. U. KHAN, S. A. MADANI, I. A. KHAN, J. KOODZIEJ, H. LI, W. LIN, K. C. YOW and C. Z. XU. Survey on blind image forgery detection. *IET Image Processing*. 2013, vol. 7, iss. 7, pp. 660–670. ISSN 1751-9659. DOI: 10.1049/iet-ipr.2012.0388.
- [4] FARID, H. Blind inverse gamma correction. *IEEE Transaction on Image Processing*. 2001, vol. 10, iss. 10, pp. 1428–1433. ISSN 1941-0042. DOI: 10.1109/83.951529.
- [5] CAO, G., Y. ZHAO and R. NI. Forensic estimation of gamma correction in digital images. In: *17th IEEE International Conference on Image Processing (ICIP)*. Hong Kong: IEEE, 2010, pp. 2097–2100. ISBN 978-1-4244-7994-8. DOI: 10.1109/ICIP.2010.5652701.
- [6] STAMM, M. C. and K. J. R. LIU. Forensic detection of image manipulation using statistical intrinsic fingerprints. *IEEE Transaction on Information Forensics and Security*. 2010, vol. 5, iss. 3, pp. 492–506. ISSN 1556-6013. DOI: 10.1109/TIFS.2010.2053202.
- [7] LIN, X., X. WEI and C. T. LI. Two Improved Forensic Methods of Detecting Contrast Enhancement in Digital Images. In: *Media Watermarking, Security, and Forensics*. San Francisco: SPIE, 2014, pp. 1–10. ISBN 978-0-819-49945-5. DOI: 10.1117/12.2038644.
- [8] CAO, G., Y. ZHAO, R. NI and X. LI. Contrast enhancement-based forensics in digital images. *IEEE Transaction on Information Forensics and Security*. 2014, vol. 9, iss. 3, pp. 515–525. ISSN 1556-6021. DOI: 10.1109/TIFS.2014.2300937.
- [9] YUAN, H. D. Identification of global histogram equalization by modeling gray-level cumulative distribution. In: *IEEE China Summit & International Conference on Signal and Information Processing*. Beijing: IEEE, 2013, pp. 645–649. ISBN 978-1-4799-1043-4. DOI: 10.1109/ChinaSIP.2013.6625421.
- [10] CHEN, Z., Y. ZHAO and R. NI. Detection for operation chain: Histogram equalization and dither-like operation. *KSII Transactions on Internet and Information Systems*. 2015, vol. 9, iss. 9, pp. 3751–3770. ISSN 1976-7277. DOI: 10.3837/tiis.2015.09.026.
- [11] PIZER, S. M., E. P. AMBURN, J. D. AUSTIN, R. CROMARTIE, A. GESELOWITZ, T. GREER, B. TER HAAR ROMENY, J. B. ZIMMERMAN and K. ZUIDERVELD. Adaptive histogram equalization and its variations. *Computer vision, graphics, and image processing*. 1987, vol. 39, iss. 3, pp. 355–368. ISSN 0734-189X. DOI: 10.1016/S0734-189X(87)80186-X
- [12] ZUIDERVELD, K. *Contrast limited adaptive histogram equalization*. San Diego: Academic Press Professional, Inc., 1994. ISBN 0-12-336155-9.
- [13] MAGUDEESWARAN, V. and J. F. SINGH. Contrast limited fuzzy adaptive histogram equalization for enhancement of brain images. *International Journal of Imaging Systems and Technology*. 2017, vol. 27, iss. 1, pp. 98–103. ISSN 0899-9457. DOI: 10.1002/ima.22214.
- [14] JUSTIN, J., J. SIVARAMAN, R. PERIYASAMY and V. R. SIMI. An objective method to identify optimum clip-limit and histogram specification of contrast limited adaptive histogram equalization for MR images. *Biocybernetics and Biomedical Engineering*. 2017, vol. 37, iss. 3, pp. 489–497. ISSN 0208-5216. DOI: 10.1016/j.bbe.2016.11.006.
- [15] OIAU, X., J. BAO, H. ZHANG, L. ZENG and D. LI. Underwater image quality enhancement of sea cucumbers based on improved histogram equalization and wavelet transform. *Information Processing in Agriculture*. 2017, vol. 4, iss. 3, pp. 206–213. ISSN 2214-3173. DOI: 10.1016/j.inpa.2017.06.001.
- [16] YADAV, G., S. MAHESHWARI and A. AGARWAL. Multi-domain image enhancement of foggy images using contrast limited adaptive histogram equalization method. In: *Proceedings of the International Conference on Recent Cognizance in Wireless Communication and Image Processing*. New Delhi: Springer, 2016, pp. 31–38. ISBN 978-81-322-2636-9. DOI: 10.1007/978-81-322-2638-3_4.
- [17] JINTASUTTISAK, T. and S. INTAJAG. Color retinex image enhancement by Rayleigh contrast limited histogram equalization. In: *International Conference on Control, Automation and Systems*. Seoul: IEEE, 2014, pp. 692–697. ISBN 978-8-9932-1507-6. DOI: 10.1109/ICCAS.2014.6987868.

- [18] YU, L., Q. HAN, X. NIU, S. M. YIU, J. FANG and Y. ZHANG. An improved parameter estimation scheme for image modification detection based on DCT coefficient analysis. *Forensic Science International*. 2016, vol. 259, iss. 1, pp. 200–209. ISSN 0379-0738. DOI: 10.1016/j.forsciint.2015.10.024.
- [19] LIN, C. S. and J. J. TSAY. Passive forgery detection using discrete cosine transform coefficient analysis in JPEG compressed images. *Journal of Electronic Imaging*. 2016, vol. 25, iss. 3. ISSN 1017-9909. DOI: 10.1117/1.JEI.25.3.033010.
- [20] LAM, E. Y. and J. W. GOODMAN. A mathematical analysis of the DCT coefficient distributions for images. *IEEE Transaction on Image Processing*. 2000, vol. 9, iss. 10, pp. 1661–1666. ISSN 1941-0042. DOI: 10.1109/83.869177.
- [21] LAM, E. Y. Analysis of the DCT coefficient distributions for document coding. *IEEE Signal Processing Letters*. 2004, vol. 11, iss. 2, pp. 97–100. ISSN 1070-9908. DOI: 10.1109/LSP.2003.821789.
- [22] NADARAJAH, S. and S. KOTZ. On the DCT Coefficient Distributions. *IEEE Signal Processing Letters*. 2006, vol. 13, iss. 10, pp. 601–603. ISSN 1558-2361. DOI: 10.1109/LSP.2006.877141.
- [23] NADARAJAH, S. Gaussian DCT Coefficient Models. *Acta Applicandae Mathematicae*. 2009, vol. 106, iss. 3, pp. 455–472. ISSN 1572-9036. DOI: 10.1007/s10440-008-9307-2.
- [24] SINGH, N., A. GUPTA and R. C. JAIN. Global Contrast Enhancement Based Image Forensics Using Statistical Features. *Advances in Electrical and Electronic Engineering*. 2017, vol. 15, no. 3, pp. 509–516. ISSN 1804-3119. DOI: 10.15598/aeec.v15i3.2189.
- [25] DUDA, R. O., P. E. HART and D. G. STORK. *Pattern Classification*. 2nd ed. New York: Wiley, 2002. ISBN 978-0-471-05669-0.
- [26] MCLACHLAN, G. and D. PEEL. *Finite Mixture Models*. New Jersey: Wiley, 2000. ISBN 978-0-471-00626-8.
- [27] LIN J. Divergence measures based on the Shannon entropy. *IEEE Transactions of Information Theory*. 1991, vol. 37, iss. 1, pp. 145–151. ISSN 0018-9448. DOI: 10.1109/18.61115.
- [28] GUPTA A. and KARMESHU. Study of compound generalized Nakagami - generalized inverse Gaussian distribution and related densities: application to ultrasound imaging. *Computational Statistic*. 2015, vol. 30, iss. 1, pp. 81–96. ISSN 0943-4062. DOI: 10.1007/s00180-014-0522-1.
- [29] MASSEY, J. F. The Kolmogorov-Smirnov test for goodness of fit. *Journal of the American statistical Association*. 1951, vol. 46, iss. 253, pp. 68–78. ISSN 0162-1459. DOI: 10.1080/01621459.1951.10500769.
- [30] SCHAEFER, G. and M. STICH. UCID: an uncompressed color image database. *Storage and Retrieval Methods and Applications for Multimedia*. San Jose: SPIE, 2004, pp. 1–9. ISBN 978-0-8194-5275-7. DOI: 10.1117/12.525375.

About Authors

Neetu SINGH Ms. Neetu Singh received her B.Tech. (Electronics and Communication Engineering) from IPEC, UP Technical University, Ghaziabad, and M.Tech. (Communication Systems and Signal Processing) from Jaypee Institute Of Information Technology (JIIT), Noida. She is pursuing her Ph.D. at JIIT, Noida. Presently working as an Assistant Professor in the Department Electronics and Communication Engineering, JIIT, Noida.

Abhinav GUPTA Dr. Abhinav Gupta received his B.Tech. (Electrical Engg.) from I.E.T., M.J.P. Rohilkhand University, Bareilly, India and M.Tech. (Signal Processing) from I.I.T. Guwahati, India. He received his Ph.D. degree from School of Computer and Systems Sciences, Jawaharlal Nehru University, New Delhi in 2013. He was a senior chief engineer at Samsung Research and Development Institute, Delhi, India. Currently, he is an Associate Professor in the Department of Electronics and Communication Engineering, JIIT, Noida, India. His research interest include signal processing, statistical modelling and machine learning. He is an author and co-author of many scientific publications.

Roop Chand JAIN Prof. R. C. Jain has been working as the Head of Department and a Professor at the Department of Electronics and Communication Engineering, JIIT, Noida, India, since 2007. He received his BE in Electronics and Communication, ME in Microwaves and Radar from the University of Roorkee, Roorkee, MEngg (Electrical Engg.) and Ph.D. (Electrical Engg.) from the University of Alberta, Canada in 1988 under commonwealth Fellowship Programme of the Govt. of India. He worked in All India Radio (AIR) and Indian Airlines Corporation (IA) from 1971-1979 and 1979-1983, respectively. He joined BITS, Pilani, Rajasthan, as a Professor in Electrical and Electronics Group in 1989.